American Heart Association | American Stroke Association

Misinterpretation of the Determinants of Elevated Forward Wave Amplitude Inflates the Role of the Proximal Aorta

Timothy S. Phan, BSBME, BSECE; John K-J. Li, PhD; Patrick Segers, PhD; Julio A. Chirinos, MD, PhD

***Background*—**The hemodynamic basis for increased pulse pressure (PP) with aging remains controversial. The classic paradigm attributes a predominant role to increased pulse wave velocity (PWV) and premature wave reflections (WRs). A controversial new paradigm proposes increased forward pressure wave amplitude (FWA), attributed to proximal aortic characteristic impedance (Z_c), as the predominant factor, with minor contributions from WRs. Based on theoretical considerations, we hypothesized that (rectified) WRs drive the increase in FWA, and that the forward pressure wave does not depend solely on the interaction between flow and Z_c (QZc product).

***Methods and Results*—**We performed 3 substudies: (1) open-chest anesthetized dog experiments (n=5); (2) asymmetric T-tube model-based study; and (3) human study in a diverse clinical population (n=193). Animal experiments demonstrated that FWA corresponds to peak QZc only when WRs are minimal. As WRs increased, FWA was systematically greater than QZc and peaked well after peak flow, analogous to late-systolic peaking of pressure attributable to WRs. T-tube modeling confirmed that increased/premature WRs resulted in increased FWA. Magnitude and timing of WRs explained 80.8% and 74.3% of the variability in the difference between FWA and peak QZc in dog and human substudies, respectively.

***Conclusions*—**Only in cases of minimal reflections does FWA primarily reveal the interaction between peak aortic flow and proximal aortic diameter/stiffness. FWA is strongly dependent on rectified reflections. If interpreted out of context with the hemodynamic principles of its derivation, the FWA paradigm inappropriately amplifies the role of the proximal aorta in elevation of FWA and PP. **(*J Am Heart Assoc*. 2016;5:e003069 doi: 10.1161/JAHA.115.003069)**

Key Words: arterial stiffness • characteristic impedance • forward wave amplitude • ventricular-arterial coupling • wave reflections

Left ventricular (LV) afterload and LV-arterial system interactions are important determinants of cardiovascular function and play a key role in various cardiovascular disease states. The pulsatile nature of LV ejection into a branching network of viscoelastic vessels encounters a vascular load that has both steady and pulsatile components. The steady load is primarily resistive in nature, comprised of the small-caliber microcirculation (peripheral resistance). The pulsatile component is complex and comprised of the spatially distributed compliant and inertial properties of the vascular tree, along with wave reflection phenomena.

There is great interest in characterizing the pulsatile phenomena that contribute to elevated pulse pressure (PP) with advancing age and various disease states, such as isolated systolic hypertension.[1–3] The prevalent view regarding changes in PP with age considers that increased pulse wave velocity (PWV), associated with vascular stiffening,[4] and the consequent earlier return of reflected waves, prominently contribute to elevated PP.[2,5–10] Recent reports from Framingham investigators have promoted a controversial viewpoint that increased forward wave amplitude (FWA), which is proposed to result from a mismatch between aortic root properties and peak aortic flow, is the predominant contributor to elevated PP with aging, with only modest contributions from wave reflections.[11–13] In steady-state conditions, peak aortic flow is sensitive to wave reflections and properties of the vascular tree distal to the aortic root.[14,15] It is therefore unlikely that the FWA paradigm is independent of distal wave reflection phenomena and specific to aortic root properties. Furthermore, the markedly increased PWV that accompanies

From Department of Electrical & Computer Engineering, Department of Biomedical Engineering, Rutgers University, Piscataway, NJ (T.S.P., J.K.L.); Cardiovascular Division, University of Pennsylvania, Philadelphia, PA (T.S.P., J.A.C.); and Biofluid, Tissue, and Solid Mechanics for Medical Applications, IBiTech, iMinds Future Health Department, Ghent University, Ghent, Belgium (P.S., J.A.C.).

Correspondence to: Timothy S. Phan, BSBME, BSECE, Hospital of the University of Pennsylvania, Cardiovascular Institute, 3400 Spruce Street. Ravdin 2, Philadelphia, PA 19104. E-mail: timphan@med.upenn.edu

Received December 1, 2015; accepted January 7, 2016.

aging should logically increase the prominence of rectified wave reflections (ie, backward waves that are rereflected at the heart, which then propagate forward).[16,17] To the best of our knowledge, there has been no systematic evaluation of the proposition that increased FWA is determined exclusively by a functional "mismatch" between peak flow and proximal aortic properties, independent of peripheral wave reflections, as has been proposed and is commonly assumed.[11,12,18,19] This distinction has important pathophysiological and therapeutic implications.

In this study, we investigated the determinants of FWA as they relate to the left ventricular-vascular system interactions that give rise to pressure and flow waves. We hypothesize that FWA is not a specific and independent marker of proximal aortic properties interacting with aortic flow,[19] but is highly dependent upon wave reflections. We assessed this issue in 3 substudies: (1) an experimental open-chest anesthetized dog model under vasoactive interventions designed to modify wave reflections; (2) a mathematical model-based study using a validated asymmetric T-tube arterial system model[20–22]; (3) a diverse clinical population of older adults with suspected or established cardiovascular disease.

Methods

Substudy 1: Animal Study

Five mongrel dogs of either sex (20–24 kg) were anesthetized with pentobarbital sodium (30 mg/kg) and ventilated through a tracheal tube with an external respirator. A left thoracotomy was performed to isolate the ascending aorta for placement of a cuff-type electromagnetic flow probe for measurement of ascending aortic flow. Ascending aortic pressure was measured with a Millar catheter-tip pressure transducer advanced from the exposed femoral artery to the site of the flow probe. Standard lead II electrocardiogram was continuously monitored. Vasoactive states were altered with intravenous infusion of methoxamine (MTX) at bolus dosages of 5 mg/mL and subsequent intravenous infusion of sodium nitroprusside (NTP) at bolus dosages of 10 mg/mL. MTX was used to increase blood pressure and wave reflections, whereas NTP was used to decrease blood pressure and abolish MTX-increased wave reflections.[23] The Rutgers University Institutional Animal Care and Use Committee approved the experimental protocols.

Substudy 2: Modeling Study

Given that experimentally modifying wave reflections through pharmacological interventions in dogs may result in a host of cardiovascular system changes (eg, heart rate [HR], cardiac output) that may confound effects of distal arterial changes, a modeling-based study was conducted to further establish the vascular determinants of FWA. The systemic arterial system was modeled as a finite PWV system represented by an asymmetric T-tube model with complex frequency-dependent loads (Figure 1).[20,21] This model consists of 2 parallel pathways, represented as elastic tubes, through which pressure and flow waves can propagate: (1) head-end and (2) body-end. The head-end pathway represents the combined circulatory path to the head and upper limbs, whereas the body-end pathway represents that of the descending aorta. Each tube is terminated in a complex load parameterized by distal compliance, viscous resistance of the vessel wall, and a terminal peripheral resistance. The asymmetric T-tube model used here has been previously validated to accurately discern between proximal and distal arterial system properties and successfully applied to various animal species and

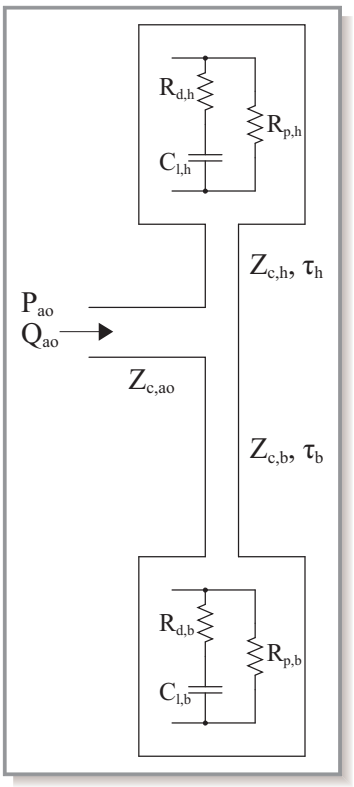

Figure 1. Asymmetric T-tube model of the arterial system. The elastic head-end (h) and body-end (b) transmission tubes are characterized by characteristic impedance ($Z_{c,h}$, $Z_{c,b}$) and wave transmission times (τ_h, τ_b). The complex frequency-dependent loads are characterized by distal load compliance ($C_{l,h}$, $C_{l,b}$), viscosity of vessel wall ($R_{d,h}$, $R_{d,b}$), and peripheral resistance ($R_{p,h}$, $R_{p,b}$).

humans.[20,21,24–28] The mathematical formulation of the model is described in detail elsewhere.[29]

The input into the model was a measured ascending aortic flow waveform typical of (1) a young adult from the study of Murgo et al.[30] and (2) an older adult from our human substudy. Initial T-tube parameters were adapted from a human study involving application of the T-tube model.[28] With input aortic flow and aortic Z_c kept constant, only the pulsatile loads of the distal circulation were modified to vary magnitude and phase (ie, intensity and timing) of distal wave reflections independent of steady afterload. Table 1 lists the parameters used for the modified asymmetric T-tube model.

Substudy 3: Human Study

Given that the animal study may not generalize well to older adults (among whom increased PP is most relevant), we studied a diverse clinical sample of human subjects comprised of a population of older adults (n=193) with suspected or established cardiovascular disease, who were referred for a cardiac magnetic resonance imaging (MRI) examination at the Corporal Michael J. Crescenz Veterans Affairs Medical Center (VAMC). Ascending aortic flow was measured with phase-contrast MRI, as previously described.[31] To avoid errors introduced by phase offset and eddy currents, we scaled the flow time integral to measured stroke volume by segmentation of steady-state free precession (SSFP) images. Arterial tonometry using high-fidelity Millar Applanation tonometers (SPT-301; Millar Instruments, Houston, TX) was performed at the carotid artery in the supine position immediately post-MRI. Brachial diastolic and mean blood pressures were used to calibrate the carotid pressure waveforms. The institutional review board of VAMC approved of the study, and all subjects provided written informed consent.

Table 1. Model Parameters for Modified Asymmetric T-Tube

	Low Reflection	Control	High Reflection
τ_h, ms	—	13.5	—
τ_b, ms	—	22.5	—
$Z_{c,h}$, mm Hg·s/mL	—	0.239	—
$Z_{c,b}$, mm Hg·s/mL	—	0.200	—
$Z_{c,ao}$, mm Hg·s/mL	—	0.108	—
$R_{P,h}$, mm Hg·s/mL	—	4.37	—
$R_{P,b}$, mm Hg·s/mL	—	1.87	—
R_P, mm Hg·s/mL	—	1.31	—
$C_{I,h}$, mL/mm Hg	+500%	0.248	−70%
$C_{I,b}$, mL/mm Hg	+500%	0.825	−70%

Percent change is relative to control. Subscripts h and b refer to the head-end and body-end tubes, respectively, and ao refers to the ascending aorta. C_I indicates distal load compliance; R_P, peripheral resistance; τ, tube transit time; Z_c, characteristic impedance.

Wave Separation Analysis

Input impedance (Z_{in}) was calculated using Fourier analysis as the ratio of measured pressure (P_m) and flow (Q_m) harmonics in the frequency domain.[9,32] As previously described,[33] aortic characteristic impedance (Z_c) was estimated in the frequency-domain by averaging the modulus of Z_{in} for harmonics 3 to 15. Only harmonics with flow magnitudes >5% of the fundamental harmonic flow magnitude were included in the averaging process to minimize the effects of noise.[33]

Forward (P_f) and backward pressure waves (P_b) were resolved in the frequency domain according to standard wave separation methods, where Q_f and Q_b are the forward and backward flow waves[9,16,34,35]:

$$P_f = \frac{P_m + Z_c Q_m}{2}; Q_f = \frac{P_f}{Z_c}$$

$$P_b = \frac{P_m - Z_c Q_m}{2}; Q_b = \frac{-P_b}{Z_c}$$

Inverse Fourier transformations were used to obtain the time-varying forward and backward waves. This standard frequency-domain method is equivalent to the time-domain method.[36,37] FWA was calculated as the maximum minus the minimum of P_f.

Comparison of P_f against the product of aortic flow and Z_c (QZc) in the time domain permits direct assessment of the degree to which P_f is modified by wave reflections, rather than a local characterization of the proximal aorta. Peak aortic flow interacting with Z_c (QZc_{max}) was calculated as the product of peak flow and Z_c. In a reflectionless arterial system, QZc_{max} is equivalent to FWA. Therefore, differences between QZc_{max} and FWA can be attributed to the influence of wave reflections on the forward wave's amplitude. Additional details are presented in the following subsection.

The complex global reflection coefficient was calculated in the frequency domain as the ratio of backward and forward waves (P_b, P_f)[34]:

$$\Gamma(j\omega) = \frac{P_b(j\omega)}{P_f(j\omega)}$$

Magnitude and timing of reflection were quantified with the modulus ($|\Gamma_n|$) and phase angle (θ_n) of Γ at harmonics of the fundamental frequency (ie, multiples of HR). The magnitude of the first harmonic of the reflection coefficient ($|\Gamma_1|$) was taken as the main measure of wave reflection magnitude.

Effect of Pulse Wave Reflection on the Forward Wave

In an arterial system with reflections, Z_{in} can be expressed in terms of characteristic impedance of the proximal aorta (Z_c) and Γ[38]:

$$Z_{in}(j\omega) = Z_c \frac{1+\Gamma(j\omega)}{1-\Gamma(j\omega)}.$$

The forward pressure wave (P_f) can be alternatively expressed in the frequency domain as a function of measured pressure (P_m) and Γ[34,38]:

$$P_f(j\omega) = \frac{P_m(j\omega)}{1+\Gamma(j\omega)}.$$

Measured pressure and flow are related through Z_{in}:

$$P_m(j\omega) = Q_m(j\omega)Z_{in}(j\omega).$$

Substitution of the expressions for Z_{in} and P_m into the expression for P_f yields:

$$P_f(j\omega) = (Q_m(j\omega)Z_c)\left(\frac{1}{1-\Gamma(j\omega)}\right).$$

Because Z_c in the proximal aorta is regarded as a purely real number in the mathematical sense,[34,38] the time-domain expression for P_f can be written in terms of a single convolution (circular convolution for the case of finite-length sampled data) between the product of Q_m and Z_c and a term related to the inverse Fourier transform (F^{-1} operator) of Γ:

$$P_f(t) = Q_m(t)Z_c * F^{-1}\left\{\frac{1}{1-\Gamma(j\omega)}\right\}$$

Any divergence in the waveforms of P_f and the product $Q_m(t)Z_c$ (hereafter referred to as QZc) as viewed in the time domain can be attributable to the transformation through the $F^{-1}\{\ldots\}$ term (ie, the effect of arterial wave reflection phenomena, per se, given that Γ is purely an arterial system characterization, much like Z_{in}[34,38,39]). It is important to acknowledge that wave reflections alter flow (Q_m) in addition to pressure; however, by focusing on the divergence of the 2 waveforms (QZc vs P_f), the $F^{-1}\{\ldots\}$ transformation can be attributed directly to arterial wave reflections (Γ). Only in the special case of no reflections will the 2 waveforms be identical (ie, $P_f(t)=Q_m(t)Z_c$).

This permits a straightforward manner to assess the degree to which characteristics of P_f (eg, amplitude, width, and so on) are manifestations of reflection phenomena, rather than local characterizations of the proximal aorta (Z_c).

Statistical Analysis

Continuous values are expressed as mean±SD or median and interquartile range, as appropriate. Proportions are expressed as percentages. Paired *t* tests were used to compare QZc_{max} versus FWA and the time of peak flow (t_{Qmax}) versus the time of peak FWA (t_{FWA}). We also compared the time integrals of QZc (TI_{QZc}) and P_f (TI_{Pf}) to assess their overall differences in morphology/amplitude. Repeated-measures ANOVA was used in the animal study to detect overall differences in hemodynamic variables in response to changes in vasoactive state. The Bonferroni correction was applied in the post-hoc pair-wise comparisons. To assess whether differences in peak amplitudes, timing to peaks, and waveform morphologies were related systematically with wave reflections, we applied multiple linear regression analysis. We considered magnitude and phase of the first 3 harmonics of the reflection coefficient ($|\Gamma_1|$, $|\Gamma_2|$, $|\Gamma_3|$, θ_1, θ_2, and θ_3) as explanatory variables given that wave reflections in the ascending aorta are concentrated primarily in the lower frequencies.[15] Step-wise linear regression analysis with backward elimination (inclusion criteria of $P<0.05$) was used to reduce the regression model to a smaller subset of explanatory variables. Standardized β regression coefficients were reported to compare the relative importance of the continuous explanatory variables examined, representing the SD change in the dependent variable for each SD change in the examined variable. All probability values are 2-tailed. Statistical significance was defined as $\alpha<0.05$. Statistical analyses were performed using Stata/MP software (14.0 for Mac; StataCorp LP, College Station, TX).

Results

Substudy 1

Separation of the measured pressure waveforms into P_f and P_b is shown in Figure 2, along with the measured aortic flow interacting with Z_c (QZc). All waveforms share a common origin to directly compare contributions to PP. In NTP-induced vasodilation, P_b was minimal, whereas MTX-induced vasoconstriction increased P_b beyond that of control. Z_c was not significantly changed by MTX and NTP (Table 2). Changes in QZc_{max} were therefore mediated primarily through changes in peak aortic flow. PP of the measured pressure is elevated greatly in MTX relative to control, in spite of the decreased contribution from QZc; MTX decreased QZc whereas P_f increased, consistent with the opposite effects that reflections have on pressure and flow. It can be appreciated that FWA corresponds to QZc_{max} only in the case of minimal reflections (NTP condition; Figure 2A). Given that wave reflections progressively increase relative to the NTP condition (ie, during the control and during MTX condition), the following phenomena are clearly appreciated: (1) There is a progressive increase in the difference between the FWA and peak flow value multiplied by Z_c; (2) there is a progressive increase in the difference between the time integral of P_f and the time integral of QZc, as indicated by the shaded red region; and (3) FWA peaks well after the time of peak flow, analogous to late-systolic peaking of measured pressure attributable to wave reflections.

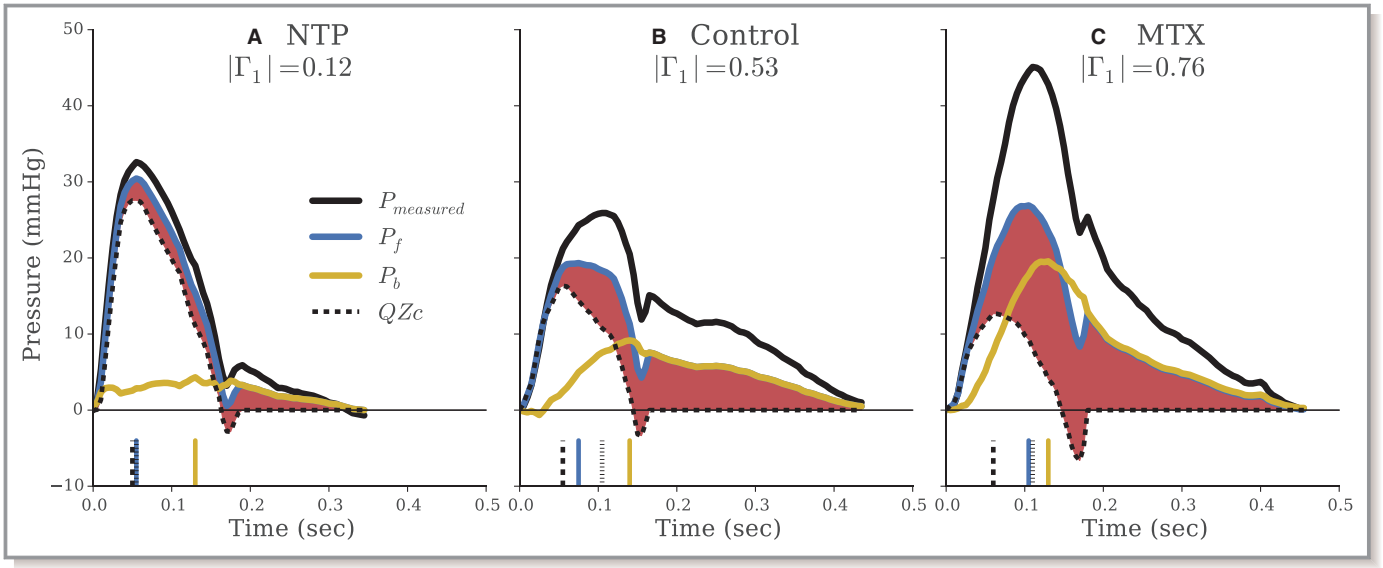

Figure 2. Pulsatile component of measured aortic pressure decomposed into forward (P_f) and backward (P_b) waves from the dog substudy. Reflection increases from (A) $|\Gamma_1|$=0.12 to (B) $|\Gamma_1|$=0.53 to (C) $|\Gamma_1|$=0.76. Measured aortic flow interacting solely with Z_c (QZc) is shown in dashed lines (—). The shaded red area represents the portion of P_f unexplained by Q×Z_c. The vertical lines at the bottom of each panel indicate timing to peak amplitudes of the corresponding line style. All waveforms are shifted to a common origin to directly compare peak amplitudes. MTX indicates methoxamine; NTP, sodium nitroprusside.

Tabulated hemodynamic variables for all dogs are listed in Table 2. In NTP-induced vasodilation, $|\Gamma_1|$ was small (0.155±0.083) and significantly reduced compared to control (0.481±0.035; *P*<0.0001). In contrast, $|\Gamma_1|$ was significantly increased by MTX (0.706±0.092) relative to control (*P*=0.0004). FWA was greater than QZc_{max}. It was only slightly greater in the NTP condition (27.8±6.2 vs 25.9±6.0 mm Hg; *P*=0.036), but was systematically greater than QZc_{max} in the control condition (20.3±1.3 vs 17.6±2.3 mm Hg; *P*=0.005) and, particularly, in the presence of increased reflections (MTX; 24.2±2.9 vs 15.3±3.0 mm Hg; *P*=0.024). Time of peak of P_f (t_{FWA}) occurred approximately at the same time as peak flow (t_{Qmax}) only in the presence of minimal reflections (NTP; difference in the timing=5±5 ms; *P*=0.089), but occurred systematically and progressively later in the presence of normal (14±5.5 ms; *P*=0.005) or increased (MTX; 55±19; *P*=0.003) reflections. Similarly, the time integral of the forward wave (TI_{Pf}) was significantly greater than the time integral of the QZc product (TI_{QZc}), with this difference increasing progressively from low to high reflection state (Table 1; *P*<0.001).

In a step-wise multiple linear regression analysis, 80.8% of the variability of the difference between FWA and QZc_{max} was explained by magnitude and phase of the reflection coefficient at the fundamental frequency, $|\Gamma_1|$ (B [standardized β]=7.542 [0.429]; 95% CI=2.38–12.7; *P*=0.008), and phase, [θ_1] (B=0.1300 [0.656]; CI=0.0718–0.188; *P*<0.001). As much as 73.6% of the variability in difference between t_{FWA} and t_{Qmax} was explained by reflection coefficient at the second harmonic of the fundamental frequency ($|\Gamma_2|$; B=0.9996 [0.858]; CI=0.0641–0.136; *P*<0.001), whereas 95% of the variability in difference between TI_{Pf} and TI_{QZc} was explained by $|\Gamma_1|$ (B=4.394 [0.976]; CI=3.80–4.99; *P*<0.001). This is consistent with reflection effects at higher harmonics being responsible for defining features such as peaks and their timing, whereas lower harmonics have greater contributions to the overall shape (and time integrals) of waves.

Substudy 2

Figure 3 shows wave separation analysis (WSA) applied to aortic pressure waveforms from the asymmetric T-tube modeling study of 3 cases for typical young (top row, Figure 3A through 3C) and old (bottom row, Figure 3D through 3F) aortic flow inputs: (1) low and late reflection ($|\Gamma_1|$=0.13; θ_1=−95.8 degrees; left column); (2) control ($|\Gamma_1|$=0.44; θ_1=−64.9 degrees; center column); and (3) high and early reflection ($|\Gamma_1|$=0.72; θ_1=−45.5 degrees; right column). With a cardiac period of 0.74 second, the fundamental (first harmonic) backward wave in the control case arrives 133 ms later than the fundamental forward wave. In the case of low and late reflections, this delay is 197 ms, and with high and early reflections, the delay is 94 ms.

Importantly, the product of aortic flow and aortic characteristic (QZc) was identical across each row, because the same aortic flow was used as input and Z_c was kept constant. Shaded red regions highlight the portion of P_f unexplained by aortic flow interacting with Z_c. In the low reflection cases (left

Table 2. Hemodynamic Variables Expressed as Mean±SD for n=5 Dogs

	NTP n=5	Control n=5	MTX n=5	*P* Value
MAP, mm Hg	69.1±11	102±16	148±13	<0.001*,†,‡
SBP, mm Hg	89.1±14	115±16	170±18	<0.001†,‡
DBP, mm Hg	58.7±11	89.4±15	131±13	<0.001*,†,‡
PP, mm Hg	30.4±7.1	25.9±1.1	38.4±6.6	0.013†
HR, bpm	166±7.5	144±22	126±9.3	0.003‡
CO, L/min	5.08±0.83	3.08±0.92	2.53±0.78	0.013*,‡
SVR, dyn·s/cm^5	3067±680	6480±907	11 150±5070	0.004‡
Z_c, dyn·s/cm^5	267.9±52.4	238.4±28.9	228.4±43.3	0.3461
$\|\Gamma_1\|$	0.155±0.083	0.481±0.035	0.706±0.092	<0.001*,†,‡
θ_1 (degrees)	−63.5±25	−68.7±16	−45.4±22	0.2414
FWA, mm Hg	27.8±6.2	20.3±1.3	24.2±2.9	0.036*
QZc_{max}, mm Hg	25.9±6.0	17.6±2.3	15.3±3.0	0.004*,‡
P value (within-condition), QZc_{max} vs FWA	0.036	0.004	0.024	
t_{FWA}, ms	59±2.2	65±7.1	121±22	<0.001†,‡
t_{Qmax}, ms	54±5.5	51±7.4	66±5.5	0.006†,‡
P value (within-condition), t_{FWA} vs t_{Qmax}	0.089	0.005	0.003	
TI_{Pf}, mm Hg·s	2.97±0.74	3.42±0.14	4.98±0.67	<0.001†,‡
TI_{QZc}, mm Hg·s	2.30±0.56	1.60±0.22	1.67±0.67	0.104
P value (within-condition), TI_{Pf} vs TI_{QZc}	0.003	<0.001	<0.001	

Comparisons across conditions were performed by repeated-measures ANOVA. CO indicates cardiac output; DBP, diastolic blood pressure; FWA, forward wave amplitude; HR, heart rate; MAP, mean arterial pressure; MTX, methoxamine; NTP, sodium nitroprusside; QZc, peak aortic flow multiplied by Zc; R_p, total peripheral resistance; SBP, systolic blood pressure; t_{FWA}, time at peak of forward wave; t_{Qmax}, time at peak flow; Γ_1, global reflection coefficient magnitude at HR.

*P<0.05 for control vs NTP.

†P<0.05 for control vs MTX.

‡P<0.05 for NTP vs MTX.

column), peak amplitude of P_f (FWA) and QZc_{max} were similar. As indicated by vertical lines at bottom of the figures, the time to peak amplitude of P_f (t_{FWA}) occurred nearly coincident with time of peak flow (t_{Qmax}). When solely the distal circulation was altered to increase the magnitude and decrease the temporal shift incurred by distal reflections, FWA was progressively greater in amplitude and occurred much later than QZc_{max}. Similarly, with increasing reflections, the overall morphology of P_f and QZc became more divergent, and the time integral of P_f was progressively greater than the time integral of QZc, as indicated by increases in shaded red areas. Consistent with the dog study and as permitted by wave transmission theory, P_f is dependent upon properties beyond the aortic root.

Substudy 3

Demographic and clinical characteristics of study subjects are presented in Table 3. The 10th, 25th, 50th, 75th, and 90th percentiles of age in the human sample were 49, 54, 62, 66, and 73 years, respectively. Examples of WSA performed in the human study are shown in Figure 4. Hemodynamic characteristics of the study subjects are presented in Table 4. Mean $|\Gamma_1|$ and θ_1 in this population was 0.44 and −53.1 degrees, respectively. With high reflections (Figure 4A and 4B), as assessed by $|\Gamma_1|$, morphology of P_f was more divergent from that of the flow Zc product (QZc), indicated by the shaded red regions. Only in minimal reflections (Figure 4C and 4D) does FWA approximate peak flow interacting with Z_c.

Dividing the subjects into tertiles of $|\Gamma_1|$, the "low" reflection group had mean $|\Gamma_1|$ of 0.33, "intermediate" mean of 0.44, and "high" mean of 0.54. FWA was not significantly different than QZc_{max} in the low reflection group (50.5±2.5 vs 49.4±2.7 mm Hg; P=0.091). Consistent with the dog and modeling studies, in the intermediate and high reflection groups, the difference was significant and systematically greater with increased reflections (intermediate: 42.3±1.7 vs 38.0±1.7 mm Hg; P<0.001; high: 41.6±1.8 vs 32.5±1.4 mm Hg; P<0.001). Similarly, peaking of P_f (t_{FWA}) occurred later than peaking of QZc (t_{QZc}) in all groups, with the

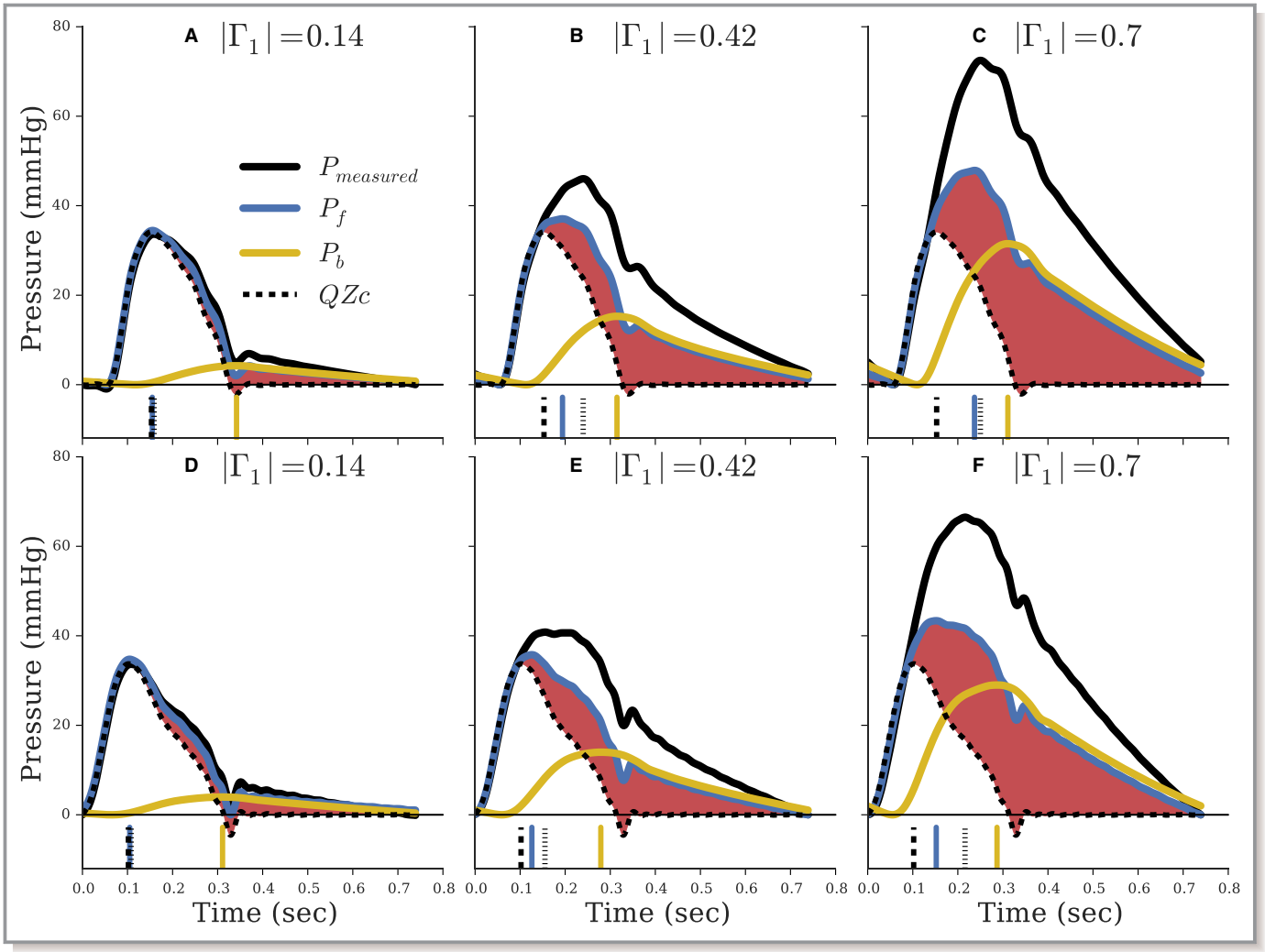

Figure 3. Waveforms from asymmetric T-tube modeling of the arterial system with input of a young adult flow waveform (A through C) and older adult (D through F). Reflection increases from $|\Gamma_1|$=0.14 (left column) to $|\Gamma_1|$=0.42 (center column) to $|\Gamma_1|$=0.70 (right column). The red shaded region indicates the portion of P_f unexplained by aortic flow interacting with Z_c. The vertical lines at the bottom of each panel indicate timing to peak amplitudes of the corresponding line style. All waveforms are shifted to a common origin to directly compare peak amplitudes.

difference in timing to peaks increasing systematically with increased reflections (low: 12.9±2.6 ms; P<0.001; intermediate: 31.0±3.4 ms; P<0.001; high: 59.6±4.9 ms; P<0.001). TI_{Pf} was systematically greater than TI_{QZc} and the difference increased systematically with increased reflections (low: 4.67±0.29 mm Hg·s; P<0.001; intermediate: 6.34±0.27 mm Hg·s; P<0.001; high: 8.56±0.43 mm Hg·s; P<0.001). Characteristics of the study subjects within each tertiles of $|\Gamma_1|$ is presented in Table 5.

Dividing the subjects into tertiles of reflection phase angle (θ_1), which is dependent on the timing of reflections, the late reflection group had mean θ_1 of −76.4 degrees, intermediate mean of −48.4 degrees, and early mean of −34.2 degrees. FWA was not significantly different than QZc_{max} in the late reflection group (45.7±2.5 vs 46.7±2.8 mm Hg; P=0.0569). Consistent with the dog and modeling studies, in the intermediate and early reflection groups, the difference was significant and systematically greater with earlier reflections (intermediate: 43.6±1.9 vs 38.4±1.8 mm Hg; P<0.001; early: 45.2±1.9 vs 34.8±1.6 mm Hg; P<0.001). Similarly, peaking of P_f (t_{FWA}) occurred later than peaking of QZc (t_{QZc}) in all groups, with the difference in timing to peaks increasing systematically with earlier reflections (late: 12.4±2.8 ms; P<0.001; intermediate: 29.5±3.5 ms; P<0.001; early: 61.8±4.5 ms; P<0.001). TI_{Pf} was systematically greater than TI_{QZc} and the difference increased systematically with earlier reflections (late: 4.29±0.25 mm Hg·s; P<0.001; intermediate: 6.67±0.27 mm Hg·s; P<0.001; high: 8.63±0.42 mm Hg·s; P<0.001).

In a step-wise multiple linear regression analysis (Table 6), 74.3% of the variability in the difference between FWA and QZc_{max} was explained by $|\Gamma_3|$ (P=0.001), θ_1 (P<0.001), θ_2

Table 3. Clinical Characteristics of Study Subjects in the Human Substudy

	Clinical Sample n=193
Age, y	62 (54.5–66)
Male sex	178 (92.2)
BMI, kg/m^2	29.8 (26.2–33.9)
Hypertension	156 (80.8)
Current smoking	61 (31.6)
Diabetes mellitus	87 (45.1)
Triglycerides, mg/dL	120 (81.0–201.0)
HDL-cholesterol, mg/dL	40 (33–48)
LDL-cholesterol, mg/dL	93 (70.5–116.0)
CAD	83 (43.0)
HF	84 (43.5)
ACE-I use	98 (50.1)
ARB use	24 (12.4)
Beta-blocker use	113 (58.5)
Long-acting nitrate use	24 (12.4)
CCB use	49 (25.4)

Values reported as median (interquartile range) or proportions expressed in percentage. ARB indicates angiotensin receptor blocker; ACE-I, angiotensin-converting enzyme inhibitor; BMI, body mass index; CAD, coronary artery disease; CCB, calcium-channel blocker; HDL, high-density lipoprotein; HF, heart failure; LDL, low-density lipoprotein.

(P<0.001), and θ_3 (P=0.005). As much as 58.9% of the variability in difference of timing to peak P_f and peak QZc was explained by $|\Gamma_2|$ (P=0.003), $|\Gamma_3|$ (P<0.001), and θ_1 (P<0.001), whereas 45.9% of the variability in difference of TI_{Pf} and TI_{QZc} was explained by $|\Gamma_2|$ (P<0.001) and θ_1 (P<0.001).

Discussion

In this study, we demonstrated that only in cases of minimal/delayed reflections does FWA primarily reveal the interaction between peak aortic flow and proximal aortic diameter/stiffness. The forward pressure wave is strongly dependent on rectified reflections, particularly in the setting of elevated PWV.[16,17] If interpreted out of context with the hemodynamic principles of its derivation, the FWA paradigm will mistakenly amplify the role of the proximal aorta in driving the increase in FWA. Our findings have important implications for our understanding of central pulsatile hemodynamics in humans and their role in health and disease.

The separation of measured pressure and flow into forward and backward waves inherently assumes a system affected by wave reflections. Implicit in the derived forward and backward waves is the occurrence of repeated reflections, such that the composite forward wave cannot be attributed to simply the initial (forward traveling) wave set up by the LV ejection.[16,34] The forward wave itself is comprised of backward waves that are rectified (ie, rereflected) at the heart end, thus becoming forward-traveling waves, as theoretically considered in the classic reference dealing with the formal derivation of the method of wave separation[34] and discussed in classic hemodynamic texts.[14,15] Rectified wave reflections result in the divergence of the forward wave morphology from that of aortic flow (and from the product of aortic flow×Zc), particularly in late systole and in diastole.[16,34,38] This is evident in our dog (Figure 2), T-tube modeling (Figure 3), and human studies (Figure 4), in which increased reflections resulted in a: (1) greater FWA relative to the product of peak flow and Z_c; (2) later peaking of the forward wave relative to peak flow; and (3) greater divergence in the morphology of the forward wave relative to product of flow and Z_c, resulting in a greater difference in their pressure-time integrals.[7,30] The fact that vasoactive stimulation (NTP, MTX), which primarily affects the distal circulation, caused variable timing to peaking of the forward wave relative to time of peak flow reveals that FWA is a much more complex parameter than simply peak flow interacting with Z_c. Analysis of changes to the amplitude and morphology of the composite forward wave as specific indicators of aortic root interactions with peak aortic flow is thus fraught with misinterpretation,[11–13,40,41] given that the important effect of rectified reflections from the distal circulation cannot be neglected.

The potential systemic effects of NTP and MTX in dogs may limit the ability to precisely resolve the primary reasons for altered forward waves, whether cardiac (eg, HR, cardiac output) or arterial system in origin.[35,42] Therefore, we complemented our animal experiments with modeling studies in which HR, stroke volume, and aortic characteristic impedance (Z_c) were kept constant. Tube transit times were kept constant, to avoid confounding by effects of pulse wave velocity on the timing of the reflected wave. Only the distal arterial loads were changed to selectively alter the distal reflection coefficients. In effect, this is equivalent to maintaining constant PWV throughout the aorta while altering the magnitude and timing of waves that come from the peripheral circulation (eg, waves that come from the iliac arteries and beyond in the case of the body-end portion of the T-tube).

Dependence of amplitude and morphology of the forward wave on the distal circulations is clearly demonstrated by T-tube modeling (Figure 3). When aortic flow and Z_c are kept constant, FWA increases when reflections from the distal circulation are altered either in intensity or timing. The morphology of the forward wave also changes because of the altered distal circulation, becoming broader in width with increased reflections that rereflect at the heart end and become forward-traveling waves.[16] Although the backward wave has typically garnered the most attention because it

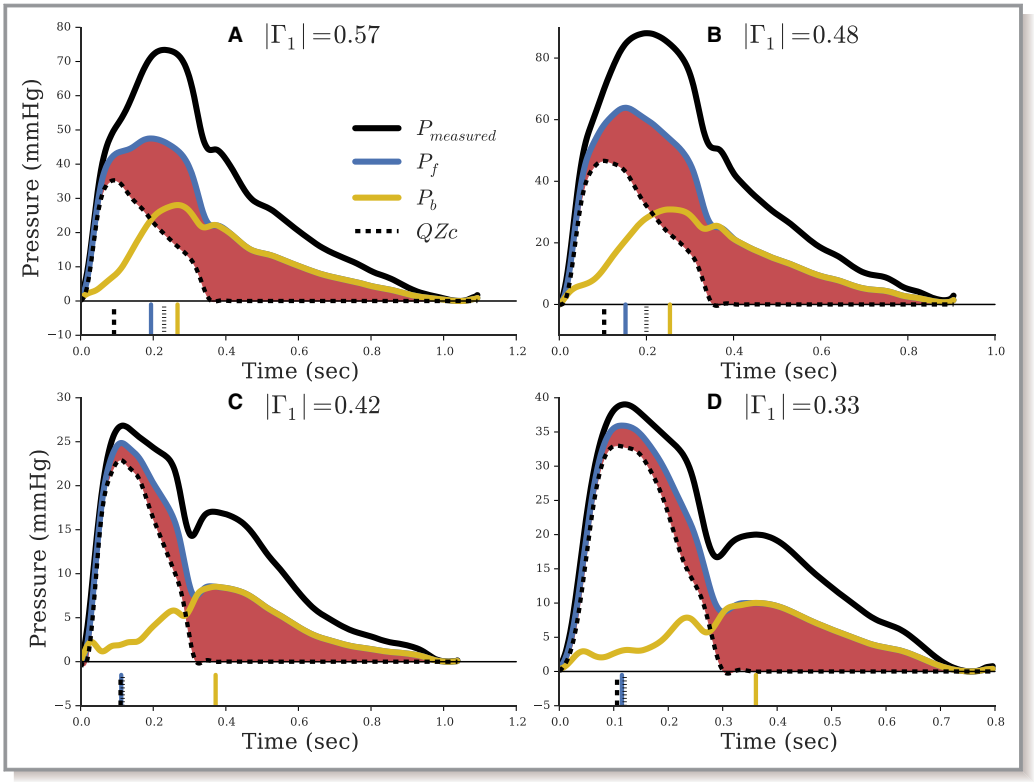

Figure 4. Pressure and flow waveforms from a human sample for high reflection ([A] $|\Gamma_1|$=0.57; [B] $|\Gamma_1|$=0.48) and low reflection ([C] $|\Gamma_1|$=0.42; [D] $|\Gamma_1|$=0.33). The red shaded region highlights portion of P_f unexplained by aortic flow interacting with Z_c. The vertical lines at the bottom of each panel indicate timing to peak amplitudes of the corresponding line style. All waveforms are shifted to a common origin to directly compare peak amplitudes.

relates to wave reflections from the distal circulation, the forward wave emerges as an informative integrated descriptor of primary waves and rectified wave reflections, rather than a specific characterization of mismatch between aortic stiffness/geometry and peak systolic flow, as proposed by the FWA paradigm.[19,43]

According to the relation from WSA[34]:

$$P_f(j\omega) = Z_c Q_f(j\omega) = Z_c \frac{Q_m(j\omega)}{1-\Gamma_G(j\omega)}$$

only when the arterial system approaches a reflection-less system ($\Gamma_G(j\omega)\rightarrow 0$) does the forward pressure wave provide information primarily about measured aortic flow interacting with Z_c that is independent of wave reflections. In contrast, during in vivo situations in which reflections are present, the forward wave is partially composed of rectified reflections. Indeed, during diastole, when inflow to the arterial system ceases, aortic pressure is composed of repeatedly rectified reflections at the closed aortic valve that give rise to the approximately exponential decay of the forward pressure wave.[44] Such effects of wave reflections on the forward wave naturally extend into the systole, as is clearly demonstrated by our results: The divergence of the forward wave morphology from that of the ejected volume flow of blood from the LV is the result of rectified reflections.[16,38] Consistent with the modeling substudy, timing of wave reflections, as assessed by phase of the fundamental harmonic of the reflection coefficient (θ_1), was the strongest predictor of the difference in FWA and QZc_{max} in both the dog and human substudies. That is, when significant effects of wave reflections occur earlier, FWA becomes elevated because of increased amount of rereflection of backward waves.

Although it is generally accepted that forward traveling waves are reflected at sites of impedance mismatches as they propagate along the arterial tree,[14,15,32,34] it is often overlooked that important impedance mismatches also occur for backward-traveling waves.[16,45] This is particularly true in the ascending aorta where backward waves will rereflect off the closed ventricular chamber during systole and the closed aortic valve in diastole.[16,34] Therefore, reports of the significant contributions of FWA to increased PP with advancing age[11–13,40,41] are not in conflict, but are rather entirely consistent, with the prevailing view that increased and/or earlier wave reflections contribute significantly to PP, rather than presenting a new fundamental mechanism. Interestingly, not only is P_f dependent on the magnitude of wave reflections,

Table 4. Hemodynamic Characteristics of Study Subjects in the Human Substudy

	Clinical Sample
	n=193
Brachial SBP, mm Hg	140 (128, 153)
Brachial SBP >140 mm Hg	92 (47.7)
Brachial DBP, mm Hg	82 (74, 90)
MAP, mm Hg	103 (94, 113)
Central SBP, mm Hg	135 (123, 150)
Central PP, mm Hg	57 (43, 65)
HR, bpm	62 (56, 71)
CO, L/min	5.09 (3.7, 6.5)
SVR, dyn·s/cm^5	1627 (1310, 2174)
Z_c, dyn·s/cm^5	114 (86, 154)
FWA, mm Hg	40.8 (33.5, 51.0)
Backward wave amplitude, mm Hg	16.5 (13.2, 21.3)
$\|\Gamma_1\|$	0.44 (0.36, 0.51)
θ_1 (degrees)	−48.0 (−64.3, −38.9)

Values reported as median (interquartile range) or proportions expressed in percentage. CO indicates cardiac output; DBP, diastolic blood pressure; FWA, forward wave amplitude; HR, heart rate; MAP, mean arterial pressure; PP, pulse pressure; SBP, systolic blood pressure; Γ_1, global reflection coefficient magnitude at HR; Z_c, characteristic impedance.

but also on its timing. It has been shown that P_f becomes broader and more peaked when PWV is increased for any given amount of reflection from the peripheries.[16,17,38] That is, when PWV is elevated, there is greater amount of repeated rereflection of waves such that P_f becomes increasingly altered. P_f therefore emerges as an integrative marker of earlier return of reflected waves (that rereflect as forward-going waves).

Our study should be interpreted in the context of its strengths and limitations. Strengths of the present study include the combination of in vivo experimental data from dogs, a mathematical model-based study using a validated model of the arterial system, and an in vivo human study. Whereas the systemic effects of MTX and NTP in dogs could not be avoided, such that potentially confounding effects on HR, LV contractility,[42] and smooth muscle tone of the proximal aorta[46] cannot be ruled out to have contributed to FWA changes, the T-tube model allowed precise control over modifications to the distal arterial load without changes to the duration and shape of LV flow ejection as well as Z_c. Furthermore, the mathematical formulation of the asymmetric T-tube model follows precisely the same governing equations upon which WSA is based. Inclusion of a wide range of clinical profiles in the human sample also supports generalization of our results to humans, including older subjects in a clinical

Table 5. Characteristics of Human Study Subjects Divided Into Tertiles by Magnitude of Reflection ($|\Gamma_1|$)

	Tertile 1	Tertile 2	Tertile 3
	n=65	n=64	n=64
Age, y	61 (52, 66)	60 (54, 66)	63 (56, 68)
Male sex	60 (92.3)	60 (93.8)	58 (90.6)
BMI, kg/m^2	31.8 (27.3, 37.0)	29.8 (26.7, 32.8)	28.1 (25.0, 30.2)
Hypertension	51 (78.5)	56 (87.5)	49 (76.6)
Current smoking	16 (24.6)	22 (34.4)	30 (46.9)
Diabetes mellitus	31 (47.7)	27 (42.2)	29 (45.3)
Brachial SBP, mm Hg	139 (126, 153)	140 (129, 150)	140 (129, 154)
Brachial SBP >140 mm Hg	32 (49.2)	29 (45.3)	31 (48.4)
Brachial DBP, mm Hg	82 (72, 90)	83 (77, 90)	82 (75, 91)
MAP, mm Hg	103 (91, 115)	103 (95, 112)	104 (95, 115)
Central SBP, mm Hg	131 (116, 148)	135 (124, 146)	141 (127, 156)
Central PP, mm Hg	49 (39, 67)	52 (46, 60)	54 (45, 73)
HR, bpm	70 (65, 78)	60 (55, 67)	59 (53, 66)
SVR, dyn·s/cm^5	1410 (1179, 1846)	1637 (1360, 1972)	1879 (1482, 2523)
Z_c, dyn·s/cm^5	124 (103, 199)	115 (91, 143)	104 (75, 137)
$\|\Gamma_1\|$	0.33 (0.31, 0.36)	0.44 (0.41, 0.47)	0.54 (0.51, 0.57)
θ_1 (degrees)	−67.4 (−83.4, −53.0)	−49.0 (−57.7, −39.9)	−36.8 (−44.7, −30.7)

Values reported as median (interquartile range) or proportions expressed in percentage. BMI indicates body mass index; DBP, diastolic blood pressure; HR, heart rate; MAP, mean arterial pressure; PP, pulse pressure; SBP, systolic blood pressure; Γ_1, global reflection coefficient magnitude at HR; Z_c, characteristic impedance.

Table 6. Relationship Between Difference in FWA and QZc_{max} vs Global Reflection Parameters in the Human Substudy

	Coefficient (Standardized β)	*P* Value
Model 1 (R^2=0.747)		
$\|\Gamma_1\|$	−0.9960 (−0.0162)	0.831
θ_1 (degrees)	0.2620 (0.8684)	<0.001
$\|\Gamma_2\|$	−4.919 (−0.0858)	0.278
θ_2 (degrees)	0.01580 (0.1642)	<0.001
$\|\Gamma_3\|$	8.885 (0.1909)	<0.001
θ_3 (degrees)	0.006278 (0.1075)	0.011
Model 2 (R^2=0.743)		
θ_1 (degrees)	0.2506 (0.8309)	<0.001
θ_2 (degrees)	0.01610 (0.1672)	<0.001
$\|\Gamma_3\|$	6.348 (0.1364)	0.005
θ_3 (degrees)	0.006666 (0.1142)	0.001

$|\Gamma_n|$ and θ_n indicate magnitude and phase (degrees) of the nth harmonic of global reflection coefficient, respectively. FWA indicates forward wave amplitude; QZc_{max}, peak aortic flow multiplied by Zc.

sample, among whom pulsatile hemodynamics is a highly relevant problem. The high consistency in our findings and conclusions across animal, modeling, and human substudies is an important aspect of our study, which increases confidence in our conclusions.

Limitations of our study include the use of carotid tonometry to obtain a surrogate of aortic pressure waveforms in our human substudy. However, carotid tonometry is a widely accepted method for central hemodynamic assessments in humans[9] and is the same method used in previous studies that assessed the FWA paradigm.[11–13] The majority of the subjects in the human study were males attributable to the demographics of the veteran patients at Veterans Affairs Medical Centers (predominance of males). However, our study addresses the hemodynamic determinants of the forward wave, and sex is not expected to play a major role. The nature of the dog experiments involving open-chest procedures and anesthesia may blunt intact physiological control systems, such that MTX- or NTP-induced LV ejection waveforms may not be representative of long-term adaptation to altered vascular loads as it occurs in humans. We did not assess the potential differences in rectified reflections in men versus women or in male versus female dogs. The potential role of sex on rectified reflections and their impact on FWA should be the focus of future research. Similarly, the role of rectified reflections in FWA in specific clinical conditions (such as systolic hypertension and heart failure) should be the focus of future research. Despite some limitations of the individual substudies, the high consistency of the findings across animal experiments, modeling studies, and human observations clearly demonstrated that the forward wave should not be interpreted simply as the initial incident wave set up by the contracting LV interacting with aortic root Z_c, given that rectified wave reflections clearly influence the forward wave amplitude and morphology.

Our dog experimental study, mathematical model-based study, and human study consistently demonstrate that FWA and morphology are dependent on properties beyond proximal aortic properties and peak aortic flow. Distal arterial properties influence the forward wave by rectified reflections. In light of the clarified role of the distal circulation in modifying forward waves, the FWA paradigm therefore reinforces the prevailing view that prominent/earlier wave reflections with advancing age are significant determinants of elevated PP, rather than proposing a new fundamental mechanism. If interpreted out of context with the hemodynamic principles of the derivation of wave separation analysis, the FWA paradigm inappropriately amplifies the role of the proximal aorta and underestimates the role of wave reflections on PP.

Sources of Funding

This research was funded by National Institutes of Health grants R56 HL-124073-01A1 (Chirinos) and 5-R21-AG-043802-02 (Chirinos), and NJMS Hemodynamics (Li).

Disclosures

None.

References

1. Westerhof N, Westerhof BE. The arterial load and its role on the heart. *Hypertension*. 2015;65:29–30.
2. Laurent S, Boutouyrie P. Recent advances in arterial stiffness and wave reflection in human hypertension. *Hypertension*. 2007;49:1202–1206.
3. Chirinos JA, Segers P, Gillebert TC, Gupta AK, De Buyzere ML, De Bacquer D, St John-Sutton M, Rietzschel ER; on behalf of the Asklepios Investigators. Arterial properties as determinants of time-varying myocardial stress in humans. *Hypertension*. 2012;60:64–70.
4. Franklin SS, Gustin W, Wong ND, Larson MG, Weber MA, Kannel WB, Levy D. Hemodynamic patterns of age-related changes in blood pressure: the Framingham Heart Study. *Circulation*. 1997;96:308–315.
5. O'Rourke MF. Wave reflections and the arterial pulse. *Arch Intern Med*. 1984;144:366.
6. Kelly R, Hayward C, Avolio A, O'Rourke M. Noninvasive determination of age-related changes in the human arterial pulse. *Circulation*. 1989;80:1652–1659.
7. O'Rourke MF, Nichols WW. Aortic diameter, aortic stiffness, and wave reflection increase with age and isolated systolic hypertension. *Hypertension*. 2005;45:652–658.
8. McEniery CM, Yasmin, Hall IR, Qasem A, Wilkinson IB, Cockcroft JR. Normal vascular aging: differential effects on wave reflection and aortic pulse wave velocity. *J Am Coll Cardiol*. 2005;46:1753–1760.
9. Segers P, Rietzschel ER, De Buyzere ML, Vermeersch SJ, De Bacquer D, Van Bortel LM, De Backer G, Gillebert TC, Verdonck PR; on behalf of the Asklepios investigators. Noninvasive (input) impedance, pulse wave velocity, and wave reflection in healthy middle-aged men and women. *Hypertension*. 2007;49:1248–1255.
10. Nichols WW, Denardo SJ, Wilkinson IB, McEniery CM, Cockcroft J, O'Rourke MF. Effects of arterial stiffness, pulse wave velocity, and wave reflections on the central aortic pressure waveform. *J Clin Hypertens*. 2008;10:295–303.

11. Torjesen AA, Wang N, Larson MG, Hamburg NM, Vita JA, Levy D, Benjamin EJ, Vasan RS, Mitchell GF. Forward and backward wave morphology and central pressure augmentation in men and women in the Framingham Heart Study. *Hypertension*. 2014;64:259–265.
12. Cooper LL, Rong J, Benjamin EJ, Larson MG, Levy D, Vita JA, Hamburg NM, Vasan RS, Mitchell GF. Components of hemodynamic load and cardiovascular events: the Framingham Heart Study. *Circulation*. 2015;131:354–361.
13. Mitchell GF, Wang N, Palmisano JN, Larson MG, Hamburg NM, Vita JA, Levy D, Benjamin EJ, Vasan RS. Hemodynamic correlates of blood pressure across the adult age spectrum: noninvasive evaluation in the Framingham Heart Study. *Circulation*. 2010;122:1379–1386.
14. Noordergraaf A. *Circulatory System Dynamics*. New York, NY: Academic Press; 1978.
15. Milnor WR. *Hemodynamics*. 2nd ed. Baltimore: Williams & Wilkins; 1989.
16. Berger DS, Li JK, Laskey WK, Noordergraaf A. Repeated reflection of waves in the systemic arterial system. *Am J Physiol*. 1993;264:H269–H281.
17. Phan TS, Khaw K, Li JK-J. Wave (Re-)reflection and pulse wave velocity determine forward wave amplitude and morphology (abstract). *J Am Soc Hypertens*. 2015;9:e32.
18. Mitchell GF, Conlin PR, Dunlap ME, Lacourciere Y, Arnold JMO, Ogilvie RI, Neutel J, Izzo JL, Pfeffer MA. Aortic diameter, wall stiffness, and wave reflection in systolic hypertension. *Hypertension*. 2008;51:105–111.
19. Mitchell GF. Arterial function. In: Berbari A, Mancia G, eds. *Arterial Disorders*. Cham: Springer International Publishing; 2015:373–383.
20. Burattini R, Campbell KB. Effective distributed compliance of the canine descending aorta estimated by modified T-tube model. *Am J Physiol*. 1993;264:H1977–H1987.
21. Shroff SG, Berger DS, Korcarz C, Lang RM, Marcus RH, Miller DE. Physiological relevance of T-tube model parameters with emphasis on arterial compliances. *Am J Physiol*. 1995;269:H365–H374.
22. Berger DS, Robinson KA, Shroff SG. Wave propagation in coupled left ventricle arterial system: implications for aortic pressure. *Hypertension*. 1996;27:1079–1089.
23. Geipel PS, Li JK-J. Nitroprusside abolishes increased arterial wave reflections from methoxamine-induced hypertension. In: Bioengineering Conference, 1989. Proceedings of the 1989 Fifteenth Annual Northeast. IEEE; 1989:131–132.
24. Berger DS, Shroff SG. On descriptive and interpretive abilities of arterial system models. In: Engineering in Medicine and Biology Society, 1995. IEEE 17th Annual Conference. Vol 1. Montreal, Quebec: IEEE; 1995:93–94.
25. Campbell KB, Burattini R, Bell DL, Kirkpatrick RD, Knowlen GG. Time-domain formulation of asymmetric T-tube model of arterial system. *Am J Physiol*. 1990;258:H1761–H1774.
26. Burattini R, Campbell KB. Comparative analysis of aortic impedance and wave reflection in ferrets and dogs. *Am J Physiol Heart Circ Physiol*. 2002;282:H244–H255.
27. Campbell KB, Shroff SG, Kirkpatrick RD, Bell DL, Taheri H. Hemodynamics of the ferret. In: Engineering in Medicine and Biology Society, 1990., Proceedings of the Twelfth Annual International Conference of the IEEE. IEEE; 1990:1158–1159.
28. Poppas A, Shroff SG, Korcarz CE, Hibbard JU, Berger DS, Lindheimer MD, Lang RM. Serial assessment of the cardiovascular system in normal pregnancy: role of arterial compliance and pulsatile arterial load. *Circulation*. 1997;95:2407–2415.
29. Burattini R, Campbell KB. Modified asymmetric T-tube model to infer arterial wave reflection at the aortic root. *IEEE Trans Biomed Eng*. 1989;36:805–814.
30. Murgo JP, Westerhof N, Giolma JP, Altobelli SA. Aortic input impedance in normal man: relationship to pressure wave forms. *Circulation*. 1980;62:105–116.
31. Chirinos JA, Rietzschel ER, Shiva-Kumar P, De Buyzere ML, Zamani P, Claessens T, Geraci S, Konda P, De Bacquer D, Akers SR, Gillebert TC, Segers P. Effective arterial elastance is insensitive to pulsatile arterial load. *Hypertension*. 2014;64:1022–1031.
32. Nichols WW, Nichols WW, McDonald DA, eds. *McDonald's Blood Flow in Arteries: Theoretic, Experimental, and Clinical Principles*. 6th ed. London: Hodder Arnold; 2011.
33. Cholley BP, Lang RM, Berger DS, Korcarz C, Payen D, Shroff SG. Alterations in systemic arterial mechanical properties during septic shock: role of fluid resuscitation. *Am J Physiol*. 1995;269:H375–H384.
34. Westerhof N, Sipkema P, Bos GCVD, Elzinga G. Forward and backward waves in the arterial system. *Cardiovasc Res*. 1972;6:648–656.
35. Quick CM, Berger DS, Noordergraaf A. Constructive and destructive addition of forward and reflected arterial pulse waves. *Am J Physiol Heart Circ Physiol*. 2001;280:H1519–H1527.
36. Li JK-J. Time domain resolution of forward and reflected waves in the aorta. *IEEE Trans Biomed Eng*. 1986;33:783–785.
37. Chirinos JA, Segers P. Noninvasive evaluation of left ventricular afterload: part 2: arterial pressure-flow and pressure-volume relations in humans. *Hypertension*. 2010;56:563–570.
38. Quick CM. Reconciling windkessel and transmission descriptions of the arterial system and the stability of muscular arteries. 1999.
39. Paul CR. *Analysis of Multiconductor Transmission Lines*. Hoboken, NJ: Wiley-Interscience; 2008.
40. Mitchell GF, Guo CY, Benjamin EJ, Larson MG, Keyes MJ, Vita JA, Vasan RS, Levy D. Cross-sectional correlates of increased aortic stiffness in the community: the Framingham Heart Study. *Circulation*. 2007;115:2628–2636.
41. Mitchell GF, Parise H, Benjamin EJ, Larson MG, Keyes MJ, Vita JA, Vasan RS, Levy D. Changes in arterial stiffness and wave reflection with advancing age in healthy men and women: the Framingham Heart Study. *Hypertension*. 2004;43:1239–1245.
42. Heyndrickx GR, Boettcher DH, Vatner SF. Effects of angiotensin, vasopressin, and methoxamine on cardiac function and blood flow distribution in conscious dogs. *Am J Physiol*. 1976;231:1579–1587.
43. Mitchell GF. Arterial stiffness: insights from Framingham and Iceland. *Curr Opin Nephrol Hypertens*. 2015;24:1–7.
44. Mynard JP, Smolich JJ. Wave potential and the one-dimensional windkessel as a wave-based paradigm of diastolic arterial hemodynamics. *Am J Physiol Heart Circ Physiol*. 2014;307:H307–H318.
45. Li JK, Melbin J, Noordergraaf A. Directional disparity of pulse reflection in the dog. *Am J Physiol*. 1984;247:H95–H99.
46. Cholley BP, Lang RM, Korcarz CE, Shroff SG. Smooth muscle relaxation and local hydraulic impedance properties of the aorta. *J Appl Physiol*. 2001;90:2427–2438.

Misinterpretation of the Determinants of Elevated Forward Wave Amplitude Inflates the Role of the Proximal Aorta

Timothy S. Phan, John K-J. Li, Patrick Segers and Julio A. Chirinos

J Am Heart Assoc. 2016;5:e003069; originally published February 19, 2016;
doi: 10.1161/JAHA.115.003069
The *Journal of the American Heart Association* is published by the American Heart Association, 7272 Greenville Avenue, Dallas, TX 75231
Online ISSN: 2047-9980